Enhancing Neuronal Coupling Estimation by NIRS/EEG Integration

Nicolás J. Gallego-Molina[1,2], Andrés Ortiz[1,2], Marco A. Formoso[1,2], Francisco J. Martínez-Murcia[2,3], and Wai Lok Woo[4]

[1] Communications Engineering Department
University of Málaga. 29004 Málaga, Spain
[2] Department of Signal Theory, Communications and Networking
University of Granada. 18060 Granada, Spain
[3] Andalusian Data Science and Computational Intelligence Institute (DaSCI)
[4] Department of Computer and Information Sciences, Northumbria University, Newcastle Upon Tyne NE1 8ST, UK njgm@ic.uma.es

Abstract. Neuroimaging techniques have had a major impact on medical science, allowing advances in the research of many neurological diseases and improving their diagnosis. In this context, multimodal neuroimaging approaches, based on the neurovascular coupling phenomenon, exploit their individual strengths to provide complementary information on the neural activity of the brain cortex. This work proposes a novel method for combining electroencephalography (EEG) and functional near–infrared spectroscopy (fNIRS) to explore the functional activity of the brain processes related to low-level language processing of skilled and dyslexic seven-year-old readers. We have transformed EEG signals into image sequences considering the interaction between different frequency bands by means of cross-frequency coupling (CFC), and applied an activation mask sequence obtained from the local functional brain activity inferred from simultaneously recorded fNIRS signals. Thus, the resulting image sequences preserve spatial and temporal information of the communication and interaction between different neural processes and provide discriminative information that enables differentiation between controls and dyslexic subjects.

Keywords: Multimodal Neuroimaging · Integrated EEG-fNIRS Analysis · Cross-Frequency Coupling · Functional Brain Activation · Dyslexia

1 Introduction

In the human brain, a vast number of neurons and their synapses work together to enable cognitive functions. This neural activity generates macroscopic brain signals by increasing the brain electrical activity, accompanied by a haemodynamic and metabolic response [4]. These direct and indirect effects of the running human brain can be measured and serve as sources for noninvasive neuroimaging techniques. Two of them are gaining popularity in the research community due to its low operating costs and ease of application: EEG and fNIRS. Having

a high temporal resolution, EEG directly measure the neural electrical activities in the cerebral cortex by detecting the induced fluctuations over the scalp. However, EEG suffers from poor spatial resolution due to volume conduction. On the other hand, with good spatial but lower temporal resolution is fNIRS. It is an optical technique that allows the study of haemodynamic responses in the brain by detecting changes in the concentration of oxygenated haemoglobin (HbO) and deoxygenated haemoglobin (HbR).

In this context, the combined use of two neuroimaging techniques is expected to surpass single-modality methods by complementing each other and exploiting their individual strengths [18, 13]. This is especially emphasised when one technique rely on the haemodynamical principle and the other on the electrophysiological principle. In this way, EEG signals are associated with the neuronal electrical activity while fNIRS signals to the haemodynamic response. Thus, integrated EEG–fNIRS approaches provide more complete information on the functional activity of the brain. These advantages arise not only from their complementary technical properties, but are also based on a physiological phenomenon called neurovascular coupling [10]. This term refers to the spatial and temporal relationship between neural activity and the regulation of cerebral blood flow. In particular, the activation of neurons within a specific brain region produce an increase of blood flow to that region to meet the augmented demand of glucose and oxygen. This results in fluctuations of haemoglobin concentrations that can be detected by fNIRS.

Impairments of neurovacular coupling has been proposed in recent works as a sign for certain neurological diseases such as Alzheimer's disease and stroke [10, 12]. Furthermore, building on the theoretical foundations of neurovascular coupling, the integration of fNIRS and EEG is attracting increasing interest in clinical and non-clinical topics [6]. In this work, we propose an integrated EEG-fNIRS approach applied to the diagnosis of Developmental Dyslexia (DD). This is a learning disability not related to mental age or inadequate schooling that impairs the learning processes of reading and spelling and affects 5–12% of the world's population [15]. We have explored the leverages of using local functional activation information from fNIRS signals to enhance the cross-frequency coupling (CFC) analysis performed on EEG signals from dyslexic and skilled readers. This approach aims to assess the presence of altered mechanisms of the neural oscillations that encode the speech signal behind the phonological deficit in DD [11] and it is based on concurrent EEG-fNIRS recordings during an experiment where participants were presented with non-interactive auditory stimuli consisting in amplitude modulated white noise at frequencies related to the core phonological units of Spanish. The rest of the paper is organized as follows. In Sect. 2, the database and methods used in this work are presented. Section 3 presents the principal results and Sect. 4, describes the conclusions and future work.

2 Materials and Methods

2.1 Dataset and Preprocessing

The data used in this work comes from a longitudinal study carried out by the LEEDUCA research group at the University of Málaga (Spain) [14], which consist of a cohort with more than 1400 children aged 4 to 8 years. It was approved by the Medical Ethical Committee of the University of Málaga (05/02/2020 PND016/2020) and with the permission of Education Office of the Junta de Andalucía to evaluate students at different public schools. Then, the quarterly application of a complete battery of cognitive and linguistic tasks to children allowed the selection of a sub-cohort for the subsequent concurrent EEG-fNIRS experiment. All selected participants are matched in age and socioeconomic index. The participants in the EEG-fNIRS sub-cohort, composed of 15 children with a clinical diagnosis of dyslexia and 29 with no obvious impairment, were presented with amplitude-modulated white noise at rates of 4.8, 16 and 40 Hz. These rates corresponds to the average production rates for core speech units in the Spanish. Each participant underwent 15-minute sessions in which the stimuli were presented sequentially in ascending and descending order for 2.5 min each ($4.8 \rightarrow 16 \rightarrow 40 \mid 40 \rightarrow 16 \rightarrow 4.8$ Hz).

EEG signals were acquired with the Brainvision actiCHamp Plus with actiCAP (Brain Products GmbH, Germany). The sampling rate was 500 Hz and its 32 electrodes follow a 10-20 configuration (auditory cortex montage). After the acquisition, the signals were baseline corrected and eye blinking artifacts were removed using blind source separation with Independent Component Analysis (ICA). Then, all channels are referenced to Cz electrode and normalized to zero mean and unit variance. In the case of fNIRS signals, the equipment used for the acquisitions was the NIRSport system with 16 optodes (eight sources and eight detectors) and a sampling frequency of 7.8125 Hz. A source-detector pair, separated by approximately 3 cm, makes up a channel; altogether we have 20 fNIRS channels per wavelength. Then, the preprocessing of the fNIRS signals has been done with the NIRSLAB software [1] including interpolation to address detector saturation, conversion of the intensity to optical density, artifact correction, transformation to hemoglobin concentration, and filtering with cut-off frequencies of 0.01 Hz and 0.09 Hz for removing artifacts of heart rate and breathing from the haemodynamic response. In addition, the placement of the electrodes, optodes and fNIRS channels over the language and auditory areas of the human brain in the EEG 10–20 system is depicted in Figure 1.

2.2 CFS Image Sequences

The EEG signals were analysed using an CFC approach. This neural mechanism intervenes in the communication and interaction between different cognitive processes that take place in different frequency bands. In addition, the coupling between different brain rhythms is proposed to reveal the neural dynamics involved in healthy and pathological brain functions [5]. In particular, we

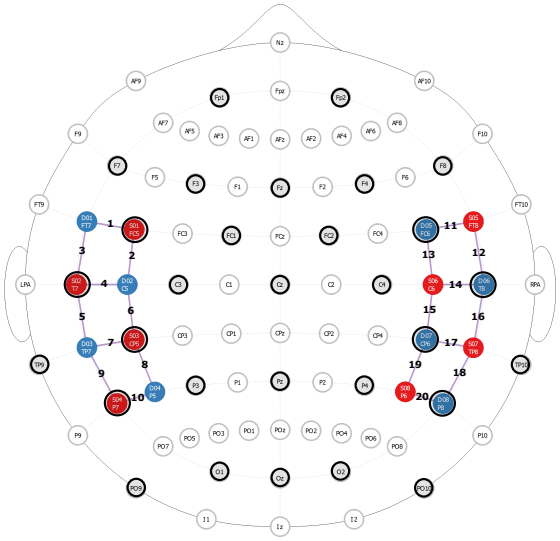

Fig. 1. Locations in the EEG 10-20 system of the EEG electrodes (gray circle with black edges), fNIRS optodes (red circles for sources and blue circles for detectors) and fNIRS channels, named from 1 to 20, are at the midpoint between a source-detector pair.

explored the cross-frequency phase synchronisation (CFS). This is also known as cross-frequency phase-phase coupling and relies on assessing the constancy of the distribution of phase-angle differences between two frequency bands

$$CFS = \left| \frac{1}{n} \sum_{t=1}^{n} e^{i(\phi_A(t) - \phi_B(t))} \right| \tag{1}$$

where n is the number of time points, and $\phi_A(t)$ and $\phi_B(t)$ are the phase angles for the frequency bands A and B.

In order to explore the temporal evolution, we measured the CFS in segments of 5 s between pairs of frequency bands (Theta: 4–8 Hz, Alpha: 8–12 Hz; Beta: 12–30 Hz; and Gamma: 30–80 Hz) at each electrode. Thus, we have 31 CFS values in each of the 30 temporal segments for each combination of frequency bands. Additionally, here we propose an approach to transform CFC information into an image sequence with the aim to preserve the spatial information of EEG electrode locations while representing the temporal development of CFS during the experiment. For this, the location of the EEG electrodes are projected from a 3-D space onto a 2-D surface [2]. Considering this 2-D surface, the CFS values computed at every segment are interpolated over a 32×32 mesh, resulting in 30 CFS images for each frequency band pair. Finally, we create three-channel CFS image sequences by combining the images obtained for three pairs of frequency bands.

2.3 fNIRS Functional Activation

Provided that the synchronisation between oscillatory processes corresponds to functional brain activity, due to neurovascular coupling, we should detect fluctuations of haemoglobin concentrations associated with this neural activation [4]. When a brain area becomes active, an increase in the metabolic demand for oxygen and glucose is observed. As a result, an oversupply of cerebral blood flow is produced and we notice an increase in HbO and a decrease in HbR in fNIRS signals from that area [16, 3]. Furthermore, it is established that the changes in HbO and HbR concentrations stemming from neural activation are negatively correlated [8, 17, 19].

$$\Delta HbR = k_F \Delta HbO \qquad with \ -1 < k_F < 0 \tag{2}$$

Therefore, we might well expect that when functional activation occurs we would measure a strong negative correlation between HbO and HbR in the haemodinamic response [7, 20]. Taking this into account, we assessed functional activation during the experiment from the fNIRS signals by calculating the Spearman correlation coefficient between 25 s segments of HbO and HbR. This duration was selected to correspond to a typical haemodynamic response [16, 3].

As we have used an fNIRS montage for the auditory cortex, this activation information only affects to the EEG electrodes placed in this area. Moreover, due to our source-detector separation, each fNIRS channel has a spatial resolution of approximately 3 cm. Thus, we can find which EEG electrodes are inside a sphere of radius 3 cm from the center point of each fNIRS channel by finding the nearest neighbours (Table 1).
Then, we have created an activation mask sequence for each subject in a similar way than explained above for the CFS image sequences. In this case, for EEG electrodes in the auditory cortex, we seek the lowest Spearman correlation coefficient from the corresponding fNIRS channels. If this coefficient is lower than a threshold (-0.9) for that segment we consider the electrode activated and assign it a 1. In other case, the electrode is not activated and we assign it a 0. For the rest of EEG electrodes as we do not have information from fNIRS we assign them a 1. In the creation of the activation mask sequence we consider the longer duration of the fNIRS segments. Therefore, one fNIRS segments correspond to five EEG segments. Finally, for each subject its own activation mask sequence is applied to its CFS image sequence.

2.4 Classification

At this point, we have an CFS image sequence with the functional activation over the auditory cortex from fNIRS for each subject. The RGB image in each frame (i.e. temporal segment) contains information from the CFS measured between the bands Theta-Gamma (R), Alpha-Beta (G) and Beta-Gamma (B). As a first approach, we used the average image over the frames for classification with pixel as feature. From each N_s samples in the LEEDUCA EEG-fNIRS dataset we get

Table 1. Nearest neighbours EEG electrodes.

fNIRS channel	Source-Detector	EEG electrodes	Hemisphere
1	S01-D01	FC5	Left
2	S01-D02	FC5	Left
3	S02-D01	T7	Left
4	S02-D02	FC5, T7	Left
5	S02-D03	T7	Left
6	S03-D02	CP5	Left
7	S03-D03	CP5	Left
8	S03-D04	CP5	Left
9	S04-D03	P7	Left
10	S04-D04	CP5, P7	Left
11	S05-D05	FC6	Right
12	S05-D06	T8	Right
13	S06-D05	FC6	Right
14	S06-D06	T8	Right
15	S06-D07	CP6	Right
16	S07-D06	T8	Right
17	S07-D07	CP6	Right
18	S07-D08	P8	Right
19	S08-D07	CP6	Right
20	S08-D08	P8	Right

an array that contains the $K = 3072$ features ($32 \times 32\ pixels \times 3\ RGB\ channels$). For the classification method we selected a machine learning technique based on ensemble of weak prediction models known as gradient tree boosting [9]. The classification is performed in a stratified K-fold cross-validation scheme with k=5, and metrics such as the Area Under the Curve (AUC) for the Receiver Operating Characteristic (ROC) curves and the balanced accuracy (BAcc) are computed.

3 Results

We have work with the LEEDUCA dataset containing concurrent EEG-fNIRS signals from an experiment where children where exposed to amplitude-modulated white noise at rates of 4.8, 16 and 40 Hz. For this preliminary approach we present the results for the 4.8 Hz stimulus, as the syllable rate is expected to emphasise the impairments in neural mechanisms that occur in DD [11]. First, the EEG signals are transformed into CFS image sequences preserving the spatial information of EEG electrode location and containing the information about the temporal development of cross-frequency phase-phase coupling in the brain. An example of these sequences is depicted in Fig. 2.a for a control subject. In this figure (Fig. 2.a) the RGB images are represented for six temporal segment of the total sequence.

Then, the fNIRS activation mask is computed for each subject considering the proximity relation between fNIRS channels and EEG electrodes from Table

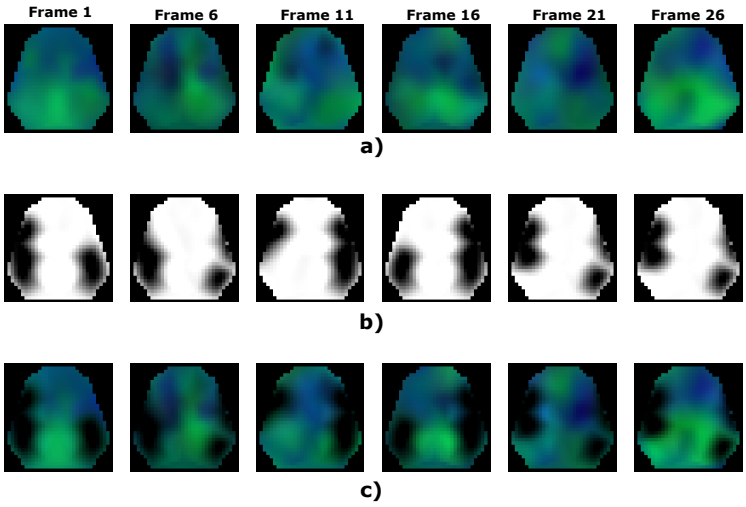

Fig. 2. Example of different image sequences for a representative control subject. a) CFS image sequence. b) fNIRS functional activation sequence. c) CFS-activation image sequence. Normalization was performed to aid visualisation.

1. The fNIRS activation sequence for a control subject is shown in Fig. 2.b, where the darker pixels correspond to deactivated zones and the whiter pixels to activated areas. In the areas outside the auditory cortex the pixels are set to 1 as we do not have functional activation information from fNIRS. Each subject's functional activation mask is then applied to their CFS image sequence, resulting in the image sequence depicted in Fig. 2.c. In these images, the CFS over the auditory cortex from the EEG signals are modified in function of their activation inferred from the fNIRS signals. Thus, we started a new path for the development of a multimodal fNIRS-EEG integration analysis approach.

In the Table 2, we have included the classifications results with gradient tree boosting considering pixels as features from the average image over the frames. In this first approach, the image sequences are extracted from the 4.8 Hz stimulus EEG and fNIRS signals and the results are presented for the CFS image sequence with and without the fNIRS functional activation mask applied. In each case, we show the average performance achieved in the five folds of cross-validation for the separated image channels and with the RGB images. Using the CFS image sequence corresponding to the channel B (which contains the information of the Beta-Gamma CFS), the classifier achieve better BAcc and AUC than combining the three channels (RGB image). However, after the application of the functional activation mask, the performance is improved for the average RGB image reaching a BAcc and AUC of 78.9%.

Finally, we conducted permutation tests to assess the statistical significance of our findings. We have created a null distribution by shuffling the labels $N_{perm} = 1000$ times and in each permutation the classifier was re-trained us-

Table 2. Classification results with gradient tree boosting.

Average image used	Channel	BAcc	Sens	Spec	AUC
From CFS image sequence	R	0.553 ± 0.069	0.4 ± 0.226	0.706 ± 0.107	0.553 ± 0.069
	G	0.648 ± 0.175	0.467 ± 0.306	0.829 ± 0.139	0.648 ± 0.175
	B	0.747 ± 0.073	0.633 ± 0.067	0.861 ± 0.091	0.747 ± 0.073
	RGB	0.695 ± 0.139	0.567 ± 0.226	0.824 ± 0.143	0.695 ± 0.139
From CFS image sequence with activation mask	R	0.582 ± 0.068	0.367 ± 0.067	0.797 ± 0.112	0.582 ± 0.068
	G	0.673 ± 0.104	0.5 ± 0.183	0.847 ± 0.111	0.673 ± 0.104
	B	0.707 ± 0.184	0.567 ± 0.271	0.847 ± 0.111	0.707 ± 0.184
	RGB	$\mathbf{0.789 \pm 0.121}$	$\mathbf{0.733 \pm 0.17}$	$\mathbf{0.845 \pm 0.126}$	$\mathbf{0.789 \pm 0.121}$

ing these shuffled label-data pairs. This is done in a five-fold cross-validation, where we evaluate the data-label link established by the classifier. Fig. 3 shows a distribution of BAcc values obtained by the classifier with the random datasets and the p-value of the BAcc score with the original dataset. The p-value is calculated as the fraction of the observed results that are greater than or equal to performance achieved with the correct labels.

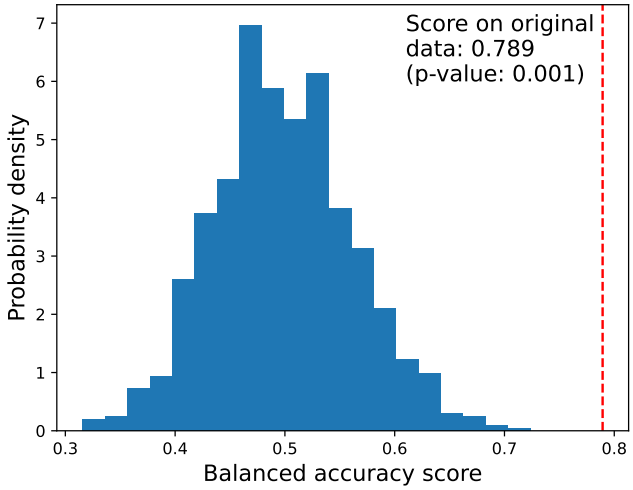

Fig. 3. Results of the permutation test. Null distribution is shown in blue.

4 Conclusions and Future Work

In this work, we propose a novel approach for a multimodal EEG-fNIRS integration that aims to take advantage of the different characteristics of these two

non-invasive neuroimaging techniques and provide more complete information on the functional activity of the brain. In order to achieve this, we rely on a concurrent EEG-fNIRS dataset arising from an experiment with non-interactive auditory stimuli presented to skilled and dyslexic seven-year-old readers. We have performed a transformation from time series data, EEG and fNIRS signals, to image sequences. Thus, preserving the information from the location of EEG electrodes and fNIRS channels and the temporal patterns of coordination of neuronal oscillations in brain functions. As a first step we have adopted an approach using pixels as features with a gradient tree boosting classifier, an efficient machine learning algorithm. Furthermore, through the application of the fNIRS functional activation masks obtained we have improved the classification performance reaching a BAcc of 78.9%.

The results obtained demonstrate the feasibility of the proposed method and provide the framework for further exploration of this line. First, the integrated EEG-fNIRS analysis can be extended to the 16 and 40 Hz stimuli to account for other origins for the deficits found in DD. In addition, the method for deriving functional activation from fNIRS signals can be improved to better match the complexity of the haemodynamic response. Finally, it is needed the exploration of feature selection techniques to improve classification performance and other machine learning algorithms that benefit more from the spatial and temporal information contained in the image sequences.

Acknowledgments This research is part of the PID2022-137461NB-C32, PID2022-137629OA-I00 and PID2022-137451OB-I00 projects, funded by the MCIN/AEI/10.13039/501100011033, by FSE+, UMA20-FEDERJA-086 (Consejería de econnomía y conocimiento, Junta de Andalucía) and by European Regional Development Funds (ERDF), as well as the BioSiP (TIC-251) research group and University of Málaga (UMA)-Campus of International Excellence Andalucía Tech. Marco A. Formoso grant PRE2019-087350 funded by MCIN/AEI/10.13039/501100011033 by "ESF Investing in your future".

References

1. NITRC: nirsLAB software. https://www.nitrc.org/
2. Bashivan, P., Rish, I., Yeasin, M., Codella, N.: Learning Representations from EEG with Deep Recurrent-Convolutional Neural Networks (Feb 2016)
3. Buxton, R.B.: Dynamic models of BOLD contrast. NeuroImage **62**(2), 953–961 (Aug 2012). https://doi.org/10.1016/j.neuroimage.2012.01.012
4. Buxton, R.B., Uludağ, K., Dubowitz, D.J., Liu, T.T.: Modeling the hemodynamic response to brain activation. NeuroImage **23**, S220–S233 (Jan 2004). https://doi.org/10.1016/j.neuroimage.2004.07.013
5. Canolty, R.T., Knight, R.T.: The functional role of cross-frequency coupling. Trends in Cognitive Sciences **14**(11), 506–515 (Nov 2010). https://doi.org/10.1016/j.tics.2010.09.001
6. Chiarelli, A.M., Zappasodi, F., Pompeo, F.D., Merla, A.: Simultaneous functional near-infrared spectroscopy and electroencephalography for monitoring of human

brain activity and oxygenation: A review. Neurophotonics **4**(4), 041411 (Aug 2017). https://doi.org/10.1117/1.NPh.4.4.041411
7. Cui, X., Bray, S., Reiss, A.L.: Functional near infrared spectroscopy (NIRS) signal improvement based on negative correlation between oxygenated and deoxygenated hemoglobin dynamics. NeuroImage **49**(4), 3039–3046 (Feb 2010). https://doi.org/10.1016/j.neuroimage.2009.11.050
8. Devor, A., Dunn, A.K., Andermann, M.L., Ulbert, I., Boas, D.A., Dale, A.M.: Coupling of Total Hemoglobin Concentration, Oxygenation, and Neural Activity in Rat Somatosensory Cortex. Neuron **39**(2), 353–359 (Jul 2003). https://doi.org/10.1016/S0896-6273(03)00403-3
9. Friedman, J.H.: Greedy function approximation: A gradient boosting machine. The Annals of Statistics **29**(5), 1189–1232 (Oct 2001). https://doi.org/10.1214/aos/1013203451
10. Girouard, H., Iadecola, C.: Neurovascular coupling in the normal brain and in hypertension, stroke, and Alzheimer disease. Journal of Applied Physiology **100**(1), 328–335 (Jan 2006). https://doi.org/10.1152/japplphysiol.00966.2005
11. Goswami, U.: A temporal sampling framework for developmental dyslexia. Trends in Cognitive Sciences **15**(1), 3–10 (Jan 2011). https://doi.org/10.1016/j.tics.2010.10.001
12. Li, R., Nguyen, T., Potter, T., Zhang, Y.: Dynamic cortical connectivity alterations associated with Alzheimer's disease: An EEG and fNIRS integration study. NeuroImage: Clinical **21**, 101622 (Jan 2019). https://doi.org/10.1016/j.nicl.2018.101622
13. Li, R., Yang, D., Fang, F., Hong, K.S., Reiss, A.L., Zhang, Y.: Concurrent fNIRS and EEG for Brain Function Investigation: A Systematic, Methodology-Focused Review. Sensors (Basel, Switzerland) **22**(15), 5865 (Aug 2022). https://doi.org/10.3390/s22155865
14. Ortiz, A., Martinez-Murcia, F.J., Luque, J.L., Giménez, A., Morales-Ortega, R., Ortega, J.: Dyslexia Diagnosis by EEG Temporal and Spectral Descriptors: An Anomaly Detection Approach. International Journal of Neural Systems **30**(07), 2050029 (Jul 2020). https://doi.org/10.1142/S012906572050029X
15. Peterson, R.L., Pennington, B.F.: Developmental Dyslexia p. 27 (2015)
16. Scholkmann, F., Kleiser, S., Metz, A.J., Zimmermann, R., Mata Pavia, J., Wolf, U., Wolf, M.: A review on continuous wave functional near-infrared spectroscopy and imaging instrumentation and methodology. NeuroImage **85**, 6–27 (Jan 2014). https://doi.org/10.1016/j.neuroimage.2013.05.004
17. Sheth, S.A., Nemoto, M., Guiou, M., Walker, M., Pouratian, N., Toga, A.W.: Linear and Nonlinear Relationships between Neuronal Activity, Oxygen Metabolism, and Hemodynamic Responses. Neuron **42**(2), 347–355 (Apr 2004). https://doi.org/10.1016/S0896-6273(04)00221-1
18. Shibasaki, H.: Human brain mapping: Hemodynamic response and electrophysiology. Clinical Neurophysiology **119**(4), 731–743 (Apr 2008). https://doi.org/10.1016/j.clinph.2007.10.026
19. Tang, L., Avison, M.J., Gore, J.C.: Nonlinear blood oxygen level-dependent responses for transient activations and deactivations in V1 — insights into the hemodynamic response function with the balloon model. Magnetic Resonance Imaging **27**(4), 449–459 (May 2009). https://doi.org/10.1016/j.mri.2008.07.017
20. Yamada, T., Umeyama, S., Matsuda, K.: Separation of fNIRS Signals into Functional and Systemic Components Based on Differences in Hemodynamic Modalities. PLOS ONE **7**(11), e50271 (Nov 2012). https://doi.org/10.1371/journal.pone.0050271